



Defense Threat Reduction Agency  
8725 John J. Kingman Road, MS-6201  
Fort Belvoir, VA 22060-6201



DTRA-TR-14-001

# TECHNICAL REPORT

## **Evaluation of Differences in Response of DOD Portable Instruments and Solid-State Detectors used by MEXT for Measurement of External Radiations with Attention to the Cosmic Radiation Component**

DISTRIBUTION A. Approved for public release: distribution is unlimited

March 2014

Prepared by:

Operation Tomodachi Registry,  
Dose Assessment and Recording Working Group

For:

Assistant Secretary of Defense for Health Affairs

This page intentionally left blank.

<b>REPORT DOCUMENTATION PAGE</b>				<b>Form Approved</b> <b>OMB No. 0704-0188</b>	
<small>Public reporting burden for this collection of information is estimated to average 1 hour per response, including the time for reviewing instructions, searching data sources, gathering and maintaining the data needed, and completing and reviewing the collection of information. Send comments regarding this burden estimate or any other aspect of this collection of information, including suggestions for reducing this burden to Washington Headquarters Service, Directorate for Information Operations and Reports, 1215 Jefferson Davis Highway, Suite 1204, Arlington, VA 22202-4302, and to the Office of Management and Budget, Paperwork Reduction Project (0704-0188) Washington, DC 20503.</small> <b>PLEASE DO NOT RETURN YOUR FORM TO THE ABOVE ADDRESS.</b>					
<b>1. REPORT DATE (DD-MM-YYYY)</b> 03-31-2014		<b>2. REPORT TYPE</b> FINAL		<b>3. DATES COVERED (From - To)</b> April 2014	
<b>4. TITLE AND SUBTITLE</b> Evaluation of Differences in Response of DOD Portable Instruments and Solid-State Detectors used by MEXT for Measurement of External Radiations with Attention to the Cosmic Radiation Component				<b>5a. CONTRACT NUMBER</b>	
				<b>5b. GRANT NUMBER</b>	
				<b>5c. PROGRAM ELEMENT NUMBER</b>	
<b>6. AUTHOR(S)</b> <sup>1</sup> Rademacher, Steven				<b>5d. PROJECT NUMBER</b>	
				<b>5e. TASK NUMBER</b>	
				<b>5f. WORK UNIT NUMBER</b>	
<b>7. PERFORMING ORGANIZATION NAME(S) AND ADDRESS(ES)</b> <sup>1</sup> Air Force Safety Center				<b>8. PERFORMING ORGANIZATION REPORT NUMBER</b>	
<b>9. SPONSORING/MONITORING AGENCY NAME(S) AND ADDRESS(ES)</b> Nuclear Technologies Department, Attn: Dr. Blake Defense Threat Reduction Agency 8725 John J. Kingman Road, Mail Stop 6201 Fort Belvoir, VA 22060-6201				<b>10. SPONSOR/MONITOR'S ACRONYM(S)</b> DTRA J9-NTSN	
				<b>11. SPONSORING/MONITORING AGENCY REPORT NUMBER</b> DTRA-TR-14-001	
<b>12. DISTRIBUTION AVAILABILITY STATEMENT</b> DISTRIBUTION A. Approved for public release: distribution is unlimited.					
<b>13. SUPPLEMENTARY NOTES</b>					
<b>14. ABSTRACT</b> This report discusses cosmic radiation and summarizes its contributions to radiation dose from external sources and the implications on measurement of external dose-rate using either pressurized ion chambers (PICs) or thallium-activated sodium iodide [NaI(Tl)]. The report finds that some NaI(Tl) systems under respond to cosmic radiation above 3 MeV deposited energy. These differences are offered as one of several contributors to the lower values of external dose rates measured by Japan's Ministry of Education, Culture, Sports, Science, and Technology (MEXT) using NaI(Tl) compared to DOD/DOE measurements using PICs. The report concludes that such limitations must be accounted for in performing assessments of dose from external sources.					
<b>15. SUBJECT TERMS</b> Operation Tomodachi, Radiation Dose, Department of Defense, Japan, Fukushima, Earthquake, Tsunami, Cosmic Radiation					
<b>16. SECURITY CLASSIFICATION OF:</b>			<b>17. LIMITATION OF ABSTRACT</b>	<b>18. NUMBER OF PAGES</b>	<b>19a. NAME OF RESPONSIBLE PERSON</b> Paul K. Blake, PhD
a. REPORT U	b. ABSTRACT U	c. THIS PAGE U	U	22 Pages	<b>19b. TELEPHONE NUMBER (Include area code )</b> (703) 767-3433

# UNIT CONVERSION TABLE

## U.S. customary units to and from international units of measurement\*

U.S. Customary Units	<div style="display: flex; align-items: center; justify-content: center;"> <div style="margin-right: 10px;"> <div style="width: 100px; height: 10px; background-color: black; position: relative;"> <div style="position: absolute; left: 0; top: -5px;">←</div> <div style="position: absolute; right: 0; top: -5px;">→</div> </div> </div> <div style="text-align: center;">             Multiply by              Divide by<sup>†</sup> </div> </div>	International Units
<b>Length/Area/Volume</b>		
inch (in)	2.54 × 10 <sup>-2</sup>	meter (m)
foot (ft)	3.048 × 10 <sup>-1</sup>	meter (m)
yard (yd)	9.144 × 10 <sup>-1</sup>	meter (m)
mile (mi, international)	1.609 344 × 10 <sup>3</sup>	meter (m)
mile (nmi, nautical, U.S.)	1.852 × 10 <sup>3</sup>	meter (m)
barn (b)	1 × 10 <sup>-28</sup>	square meter (m <sup>2</sup> )
gallon (gal, U.S. liquid)	3.785 412 × 10 <sup>-3</sup>	cubic meter (m <sup>3</sup> )
cubic foot (ft <sup>3</sup> )	2.831 685 × 10 <sup>-2</sup>	cubic meter (m <sup>3</sup> )
<b>Mass/Density</b>		
pound (lb)	4.535 924 × 10 <sup>-1</sup>	kilogram (kg)
atomic mass unit (AMU)	1.660 539 × 10 <sup>-27</sup>	kilogram (kg)
pound-mass per cubic foot (lb ft <sup>-3</sup> )	1.601 846 × 10 <sup>1</sup>	kilogram per cubic meter (kg m <sup>-3</sup> )
Pound-force (lbf avoirdupois)	4.448 222	Newton (N)
<b>Energy/Work/Power</b>		
electronvolt (eV)	1.602 177 × 10 <sup>-19</sup>	joule (J)
erg	1 × 10 <sup>-7</sup>	joule (J)
kiloton (kT) (TNT equivalent)	4.184 × 10 <sup>12</sup>	joule (J)
British thermal unit (Btu) (thermochemical)	1.054 350 × 10 <sup>3</sup>	joule (J)
foot-pound-force (ft lbf)	1.355 818	joule (J)
calorie (cal) (thermochemical)	4.184	joule (J)
<b>Pressure</b>		
atmosphere (atm)	1.013 250 × 10 <sup>5</sup>	pascal (Pa)
pound force per square inch (psi)	6.984 757 × 10 <sup>3</sup>	pascal (Pa)
<b>Temperature</b>		
degree Fahrenheit (°F)	[T(°F) - 32]/1.8	degree Celsius (°C)
degree Fahrenheit (°F)	[T(°F) + 459.67]/1.8	kelvin (K)
<b>Radiation</b>		
activity of radionuclides [curie (Ci)]	3.7 × 10 <sup>10</sup>	per second (s <sup>-1‡</sup> )
air exposure [roentgen (R)]	2.579 760 × 10 <sup>-4</sup>	coulomb per kilogram (C kg <sup>-1</sup> )
absorbed dose (rad)	1 × 10 <sup>-2</sup>	joule per kilogram (J kg <sup>-1§</sup> )
equivalent and effective dose (rem)	1 × 10 <sup>-2</sup>	joule per kilogram (J kg <sup>-1**</sup> )

\* Specific details regarding the implementation of SI units may be viewed at <http://www.bipm.org/en/si/>.

† Multiply the U.S. customary unit by the factor to get the international unit. Divide the international unit by the factor to get the U.S. customary unit.

‡ The special name for the SI unit of the activity of a radionuclide is the becquerel (Bq). (1 Bq = 1 s<sup>-1</sup>).

§ The special name for the SI unit of absorbed dose is the gray (Gy). (1 Gy = 1 J kg<sup>-1</sup>).

\*\* The special name for the SI unit of equivalent and effective dose is the sievert (Sv). (1 Sv = 1 J kg<sup>-1</sup>).

**DTRA-TR-14-001: Evaluation of Differences in Response of DOD Portable Instruments  
and Solid-State Detectors used by MEXT for Measurement of External  
Radiations with Attention to the Cosmic Radiation Component**

## **Table of Contents**

List of Figures .....	ii
List of Tables .....	ii
Section 1. Introduction .....	1
Section 2. Background .....	2
Section 3. Differences in Response of NaI(Tl) and PICs.....	8
Section 4. Conclusions .....	15
Section 5. References .....	16

## List of Figures

Figure 1. MEXT monitoring of external dose at Shinyuku Ward, Tokyo Prefecture.....	4
Figure 2. MEXT monitoring of external dose at Aomori Prefecture.....	4
Figure 3. MEXT monitoring of external dose at Yamaguchi Prefecture .....	5
Figure 4. Mass stopping power for muons in NaI(Tl) from equation 4.7 of Turner (1992) .....	9
Figure 5. Integral fluxes averaged over the 11-year solar cycle for muons ( $\mu$ ), electrons ( $e$ ), protons ( $p$ ), and photons ( $ph$ ) arriving at geomagnetic latitudes~ $40^\circ$ vs. their kinetic energy, Figure 1 from Cecchini and Spiro (2012).....	9
Figure 6. Cumulative distribution function (CDF) for random particle transversals through a right circular cylinder of height and diameter = 5.08 cm, and ratio of path length, L, to diameter, D .....	10
Figure 7. Example photon interaction and muon transversals through right circular cylinder with diameter and height equal to 5.08 cm, i.e., 2 inch by 2 inch.....	11
Figure 8. Estimated differences in external dose rates of an ion chamber and a 2 inch by 2 inch NaI(Tl) for fixed cosmic radiation levels at four altitudes in the presence of three different terrestrial contributions .....	13

## List of Tables

Table 1. Effective dose rate at various altitudes for individual particle and ray groups based on calculations of Goldhagen (2000) .....	3
Table 2. Descriptive statistics for MEXT monitoring stations that were not significantly impacted by FDNPS releases, March 14–May 13, 2011 .....	6
Table 3. Detector responsiveness to radiations in the cosmic spectrum .....	8
Table 4. Data from Table 2 modified with respective detector response characteristics .....	12

## Section 1.

### Introduction

Department of Defense (DOD) measurements of external radiation using portable instruments during Operation Tomodachi (OT) had higher values compared to results reported by Japan's Ministry of Education, Culture, Sports, Science, and Technology (MEXT) for its monitoring stations at similar geographical locations. External radiation monitoring performed by MEXT and other Japanese entities provided vital augmentation to DOD measurements in dose assessments performed by the Dose Assessment and Recording Working Group (DARWG)<sup>1</sup> and documented in Cassata et al. (2012). Hence, it was important to understand the sources of those differences, which were attributed to a number of factors.

First, many of the MEXT stations were located on the tops of buildings, while DOD measurements were typically collected at a height of one meter above ground level. Second, a comparison of measurements obtained with DOD portable pressurized ion chambers (PIC) and energy-compensated Geiger-Mueller (G-M) detectors demonstrated that G-M measurements were likely to be biased-high by a factor of two at low external dose rates, while measurements by the PIC at low external dose rates could also be biased high if measurements were collected in the rate mode. The bias in the PIC is attributed to the varying dose rate values reported on the digital display, which requires operators to select a value for reporting that can be influenced by the natural tendency for some operators to report the highest displayed values. This will cause a high bias in reported results that is operator-induced. Third, an under-response of MEXT solid-state scintillators, such as thallium-activated sodium iodide [NaI(Tl)], to cosmic radiation has been explored as a potential source of bias. Cosmic radiation contributes to external radiation exposure. Its magnitude is dependent on the solar activity, altitude, and geomagnetic latitude. The magnitude of this source of bias for a given measurement location is difficult to quantify with high precision because the radiation environment that existed during Operation Tomodachi cannot be re-created, and the details on the collections of DOD measurements were not sufficient to completely characterize exact locations, detector configurations, or environmental conditions. The first two sources of bias—detector mounting location and operator-induced selection of high readings—were discussed in detail in Cassata et al. (2012). This report discusses the third possible source of bias from under-response of MEXT detection systems to cosmic radiation.

---

<sup>1</sup> The Dose Assessment and Recording Working Group (DARWG) is one of four working groups of DOD's Operation Tomodachi Registry (<http://registry.csd.disa.mil/otr>).

## Section 2.

### Background

Under normal conditions, the external radiation environment comprises cosmic radiation (cosmic rays and solar particles)<sup>2</sup> and radiations emitted from radioactive material in the terrestrial environment. In general, for most outdoor locations at or near ground level, the largest source of terrestrial radiation comes from soil, with the exception of paved areas or areas adjacent to buildings, where the composition of building materials influences instrumental measurements. The magnitude of external radiation is primarily a function of altitude and geomagnetic latitude for the cosmic source, while the terrestrial portion is related to composition and concentrations of radioactive materials in the local environment. These materials are naturally-occurring and man-made. The most important naturally-occurring radioactive materials in the environment are <sup>232</sup>Th (and radioactive decay products), <sup>238</sup>U (and radioactive decay products), and <sup>40</sup>K. Other naturally-occurring radioactive materials include <sup>235</sup>U (and decay products), <sup>87</sup>Rb, and numerous ones produced by cosmic rays in the atmosphere (i.e., <sup>3</sup>H, <sup>7</sup>Be, and <sup>14</sup>C). Man-made radionuclides, such as those released from industrial processes, accidents, atmospheric testing of nuclear weapons, etc., are considered part of the terrestrial source.

At sea level, muons are the most abundant type by number of charged particle in the cosmic spectrum and are also responsible for the greatest contribution to the calculated effective dose. At about 8,500 feet altitude, the contribution to effective dose from neutrons is about the same as that from muons for calculations near the polar plateau as calculated by Goldhagen (2000). Table 1 contains effective dose rates at sea level, 2,500, 5,000, and 7,500 feet for the various cosmic radiations, based on calculations from Goldhagen (2000). For this sea level example, 80% of the effective dose is from muons. Generally, for increasing geomagnetic latitudes up to the Polar Regions, galactic cosmic ray intensities increase due to the reduction in geomagnetic strength and subsequent acceptance of lower momentum galactic cosmic rays. At some point, called the polar plateau, the intensity of galactic cosmic rays does not increase with increasing geomagnetic latitude, because lower momentum galactic cosmic rays, deflected by the solar wind, would not be available for penetration through the earth's magnetic field. The assessment of effective dose from the cosmic spectrum cannot be accomplished using a single measurement instrument because of the complex mixture of particles and the application of radiation weighting factors. As such, effective dose is commonly based on estimated contributions from neutrons, combined with the directly ionizing radiations and photons measured with a PIC or other suitable instrument. Assessment of the directly ionizing radiations and photons from cosmic origin is confounded by contributions from terrestrial radiation, because most common instruments used to measure external radiation do not have the capability to distinguish the sources of radiation for individual interactions.

---

<sup>2</sup> Cosmic rays are very high-energy particles, mainly originating outside the solar system. They may produce showers of secondary particles that penetrate and impact earth's atmosphere and sometimes reach the surface. The term "ray" is an historical accident, as cosmic rays were initially incorrectly thought to be electromagnetic radiation.



Historically, most external radiation measurements have been conducted with PICs, where the detection system responds to photons and directly ionizing radiations, i.e., electrons, muons, pions, protons, heavy charged particles, etc. Energy-compensated G-Ms and solid-state scintillators, i.e., NaI(Tl), have been used more commonly in the last couple of decades for external radiation monitoring. With respect to external radiation monitoring during the FDNPS nuclear reactor accident, accurate assessment of external radiation from cosmic particles and photons was not critical to health and safety evaluations, beyond the fact that they were properly accounted for in assessment of the pre-accident radiation environment.

**Table 1. Effective dose rate at various altitudes for individual particle and ray groups based on calculations of Goldhagen (2000)**

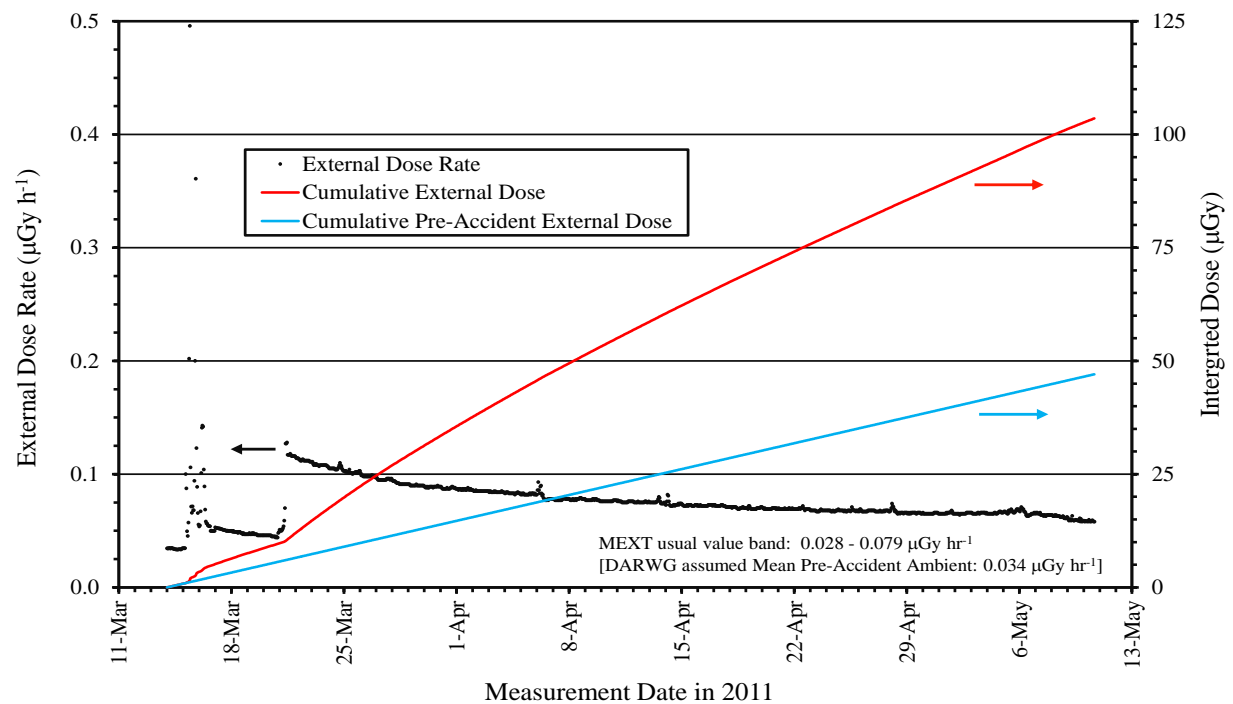
Cosmic Radiation Type	Dose Rate ( $\mu\text{Sv hr}^{-1}$ )			
	Sea-Level	2,500 ft	5,000 ft	7,500 ft
Muons	0.027	0.031	0.036	0.0405
Pions	*	-	0.00066	0.0011
Protons	0.0004	0.0012	0.0027	0.005
Photons & Electrons	0.0042	0.0069	0.01	0.013
Neutrons	0.0036	0.0089	0.019	0.036
Total	0.035	0.049	0.069	0.1

\* Negligible

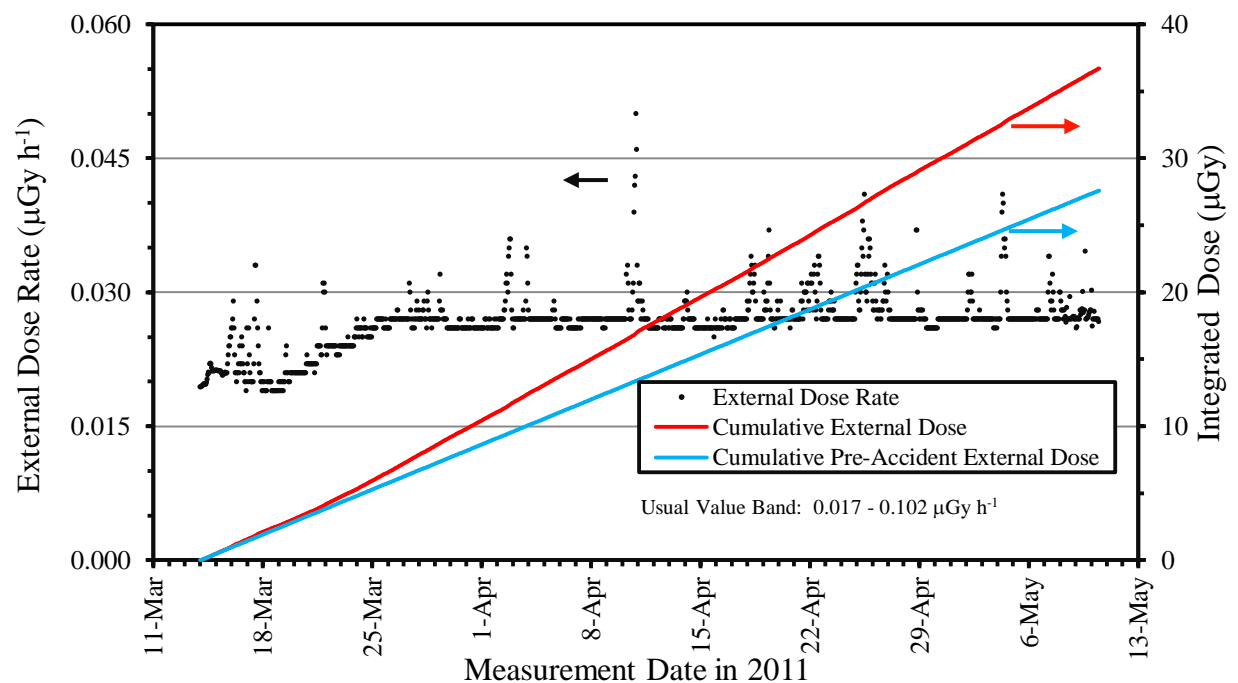
However, the differential response of various instruments to cosmic radiation made comparisons of data sets difficult due to the potential for different pre-accident background external dose rates. MEXT monitoring stations had extensive pre-accident monitoring data that were reported along with data collected after the releases from the Fukushima Daiichi Nuclear Power Station (FDNPS) began contributing to the measurements. Unfortunately, DOD and DOE measurements do not have accompanying pre-accident external radiation measurements because these systems were not commonly used for environmental measurements. As such, there is no basis for comparison of pre-accident measurements of external radiation by MEXT monitoring stations with DOD and DOE measurements. Figure 1 displays results of MEXT monitoring of external dose rates at the Shinyuku Ward, Tokyo Prefecture for the period between March 14 and May 10, 2011. The cumulative dose over the period is shown by the red line, while the blue line is an estimate of cumulative external dose from background, assuming a background dose rate of  $0.034 \mu\text{Gy h}^{-1}$ . MEXT reported the “usual value band” for this measurement location as  $0.028$  and  $0.079 \mu\text{Gy h}^{-1}$ . Apparent from the plot are the initial detections of FDNPS releases on March 14.

Figure 2 is a dose-rate plot for Aomori Prefecture, which is north of FDNPS, and experienced much lower contributions to dose rate from the releases than Tokyo Prefecture. The net cumulative dose over the March 14–May 10 period displayed is  $9.1 \mu\text{Gy}$ , while that for Tokyo Prefecture is  $56.4 \mu\text{Gy}$ ; over six-fold higher. Assessment of the net cumulative dose required assumptions regarding the pre-accident external exposure rate results. MEXT reported these in terms of the “usual value band,” which is displayed on Figure 1 and Figure 2. Fluctuations in reported pre-accident exposure rates are believed to be primarily from the

random nature of radioactive decay and variability in ground-surface deposition of radon progeny.



**Figure 1. MEXT monitoring of external dose at Shinyuku Ward, Tokyo Prefecture**



**Figure 2. MEXT monitoring of external dose at Aomori Prefecture**

The plot in Figure 3 provides a good representation of the fluctuations of external radiation at a MEXT monitoring site in Yamaguchi Prefecture that did not experience significant contributions from the FDNPS releases, because it was located over 500 miles from the station.

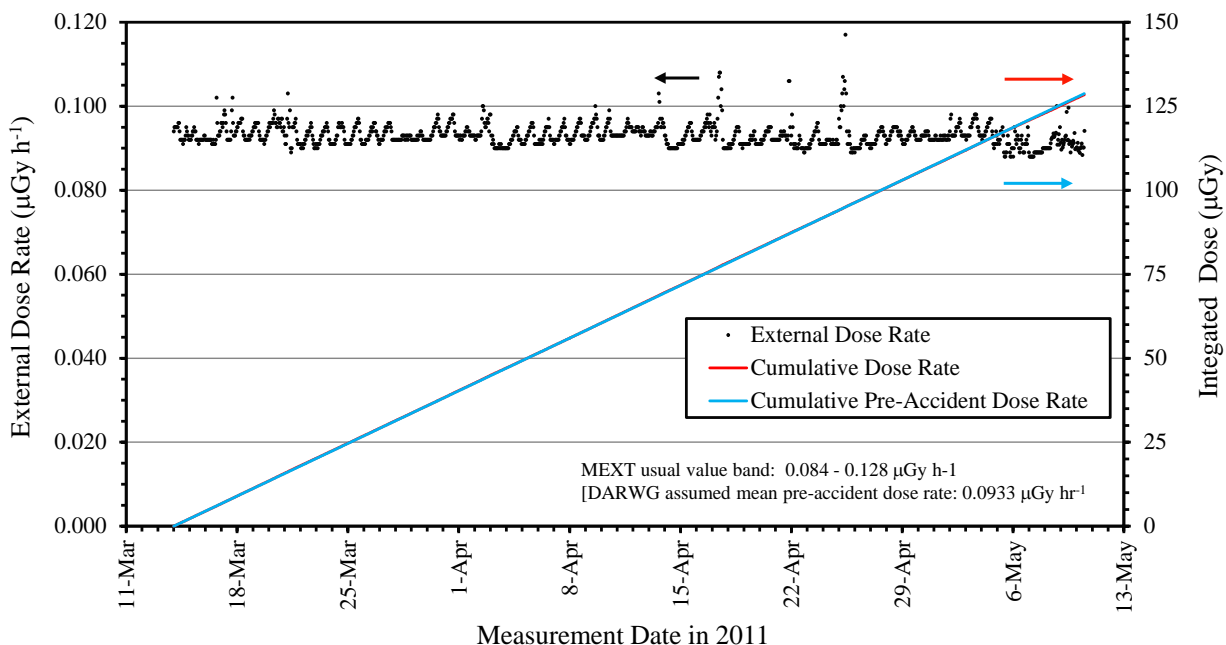


**Figure 3. MEXT monitoring of external dose at Yamaguchi Prefecture**

One noticeable effect of the insignificant contribution to dose rates from FDNPS releases is the apparent superposition of the cumulative pre-accident dose rate (blue line) and the cumulative dose rate (red line) in Figure 3. For this site, the mean dose rate calculated from the displayed rates was  $0.0933 \mu\text{Gy hr}^{-1}$ , with minimum and maximum reported hourly dose rates of  $0.084$  and  $0.128 \mu\text{Gy hr}^{-1}$ . Obvious from the figure, the vast majority of the measured data points are clustered near the mean with intermittent high recorded values. The mean of the distribution is much closer to the minimum of the range than the maximum, and the distribution of dose rates is skewed to the right. This characteristic is expected for all of the MEXT data sets regarding the mean pre-accident exposure rate with respect to the “usual value band” that accompanied every data set. Evidence exists that the intermittent high external exposure values are largely associated with increases in surface-deposited radon progeny that is promoted by atmospheric pressure changes and rainout of radon progeny. Nagaoka et al. (2012) demonstrates this effect in dose rate variations with time for Chiba prefecture in March 2011.

There was considerable variability in the average external dose rates at MEXT monitoring stations that were not significantly impacted by FDNPS releases. Descriptive statistics for four stations for the period of March 14 to May 13 are listed in Table 2. The mean external dose rates ranged from  $0.0293$  to  $0.0933 \mu\text{Gy h}^{-1}$ . Under the premise of this report that MEXT NaI(Tl) systems record very little of the total contributions from the cosmic spectrum to external exposure, the range represents predominantly that from terrestrial photons.

**Table 2. Descriptive statistics for MEXT monitoring stations that were not significantly impacted by FDNPS releases, March 14–May 13, 2011**

Location		MEXT “Usual Value Band” ( $\mu\text{Gy h}^{-1}$ )		Descriptive Statistics for Hourly Measurements ( $\mu\text{Gy h}^{-1}$ )				
Prefecture	City	Lower	Upper	Minimum	Maximum	Mean	Median	St Dev
Nara	Nara	0.046	0.080	0.046	0.061	0.0483	0.048	0.0016
Hiroshima	Hiroshima	0.035	0.069	0.045	0.059	0.0479	0.047	0.0021
Yamaguchi	Yamaguchi	0.084	0.128	0.088	0.1170	0.0933	0.093	0.0026
Nagasaki	Omura	0.027	0.069	0.027	0.045	0.0293	0.029	0.0016

Based on 4,300 in-situ  $\gamma$ -radiation measurements of primordial radionuclides in surface soils, Minato (2006) estimated terrestrial  $\gamma$ -radiation dose rates throughout Japan at a meter above ground level. Isodose contours were developed for Japan with contour increments of  $10 \mu\text{Gy h}^{-1}$  from 20–30 to 90–100,  $< 20$ , and  $> 100 \mu\text{Gy h}^{-1}$ . For the four locations with MEXT station results displayed in Table 2, the range of mean external exposure rates is consistent with those reported by Minato (2006). As well, for other measurement locations that were impacted by FDNPS fallout, estimated pre-accident average background dose rates of the MEXT systems were on par with the estimated terrestrial dose rates for the general location. It is important to note that the work by Minato does not include man-made contributions to the terrestrial radiation source, which prior to FDNPS would have been small at the locations assessed.

Use of NaI(Tl) detectors to characterize terrestrial photon emissions and their associated external dose is common among Japanese investigators. In work investigating terrestrial gamma radiation dose in Kochi prefecture (Chikasawa et al. 2001), the investigator noted a high correlation in external dose rates measured by a NaI(Tl) with those estimated for soil with known concentrations of  $^{40}\text{K}$ , the thorium series, the uranium series, and  $^{137}\text{Cs}$ . Nagaoka (1987) compared methods for assessment of terrestrial exposure rates in high-purity germanium and NaI(Tl) detectors, where the response of each system was truncated at 3 MeV per energy deposition event. While the paper’s primary purpose was to illustrate the good agreement between the two systems for measurements in the same environment, the authors noted, “the cosmic ray exposure rate below 3 MeV is small (about 2–5 % of  $\gamma$  exposure rate in a typical environment) . . .” The authors of this work used multiple NaI(Tl) systems with crystals ranging in size from a 3 inch by 3 inch right cylinder to a five-inch diameter sphere. For a number of the MEXT monitoring stations, it is implausible that the NaI(Tl) systems were responsive to a significant fraction of directly ionizing particles and photons in the cosmic spectrum in the cosmic spectrum. Nagaoka (2008) measured the neutron dose rates with a high sensitivity radiation equivalent man (REM) counter and directly-ionizing, cosmic particles plus photons with an ionization chamber/NaI(Tl) combination at 240 locations in Japan. The dose rates from directly-ionizing particles plus photons from a cosmic source ranged from about 0.030 to  $0.068 \mu\text{Gy h}^{-1}$ , with the high value on Mount Fuji at an elevation of 2,400 m (7,900 feet). The average was about  $0.031 \mu\text{Gy hr}^{-1}$ , and very close to the minimum, as the vast majority of measurement locations were close to sea level. The range of values across the respective elevations are very similar to those listed in Table 1, though some differences between the two data sets due to differences in solar activity and the geomagnetic latitude are to be expected. The

assumed mean pre-accident dose rate for the MEXT Aomori Prefecture NaI(Tl) monitor was  $0.020 \mu\text{Gy h}^{-1}$ , which is substantially lower than the minimum dose rate from directly-ionizing particles plus photons from cosmic origin of  $0.030 \mu\text{Gy h}^{-1}$ . Among the 47 MEXT monitoring stations, 17 had a lower value of the “usual value band” below  $0.030 \mu\text{Gy h}^{-1}$ . The lowest was only  $0.013 \mu\text{Gy h}^{-1}$  for the MEXT station on Okinawa Island. Minato (2006) excluded Okinawa Island.

## Section 3.

### Differences in Response of NaI(Tl) and PICs

This report focuses on potential differences between a PIC and NaI(Tl), because MEXT stations were equipped with NaI(Tl) detectors, while many DOD and DOE measurements were performed with PICs. Table 3 contains a summary of the responsiveness of each instrument to cosmic particles and rays. In the case of the ion chamber, the detector will respond to all of the particles, with the exception of neutrons where the response will be negligible. Most detection systems cannot appropriately translate dose created from some particles into effective dose. For example, muons, pions, and the secondary electrons from photon interactions have a radiation

**Table 3. Detector responsiveness to radiations in the cosmic spectrum**

Radiation Type	Detector Responsiveness	
	Ion Chamber	NaI(Tl)*
Muons	Yes	Small fraction of events
Pions	Yes	Small fraction of events
Protons	Yes (but no $w_r$ correction of 2)	Small fraction of events
Photons & Electrons	Yes	Yes (but small fraction of events for cosmics)
Neutrons	Negligible	Negligible

\* Maximum energy threshold for acceptance at 3 MeV

weighting factor,  $w_r$ , of 1 and will produce a valid dose estimate from detector response. In the case of protons, however, effective dose from proton interactions will be underestimated, as proton interactions in most detection systems are indiscriminate from electrons, photons, etc. Goldhagen (2000) applied a  $w_r$  of 2, consistent with National Council on Radiological Protection and Measurements Report 116 (NCRP, 1993). For example, PICs, as currently configured, do not associate a detector response with a specific interaction; therefore, the  $w_r$  of 2 cannot be applied to the proton contribution to dose. In contrast, however, because most solid-state detection systems have a user-set upper limit on energy deposition of quantified events, most cosmic particle interactions are not recorded, essentially being truncated from the dose reported by these devices. MEXT NaI(Tl) systems truncated events whose energy deposition was greater than 3 MeV. This practice substantially limited quantification of dose from muon, pion, electron, and proton interactions in the sensitive volume to only those events whose particle traversal path lengths were a small fraction of the maximum possible path length.

To illustrate this point, energy deposition for individual charged particles using the product of mass stopping power and the distribution of possible chord lengths from random particle traversals through the sensitive volume of the NaI(Tl) detector is evaluated. An example of mass stopping power for muons in NaI(Tl) is shown in Figure 4, based on equation 4.7 of Turner (1992) and estimated minimum stopping powers in NaI(Tl) from Groom et al. (2001). The mass stopping power is high for muons of low kinetic energy and reaches a minimum at around 100 to 200 MeV. A plot of integral fluxes averaged over the 11-year solar cycle for

muons, electrons, protons, and photons versus their kinetic energies is contained in Figure 5, which is reproduced from Cecchini and Spuiro (2012).

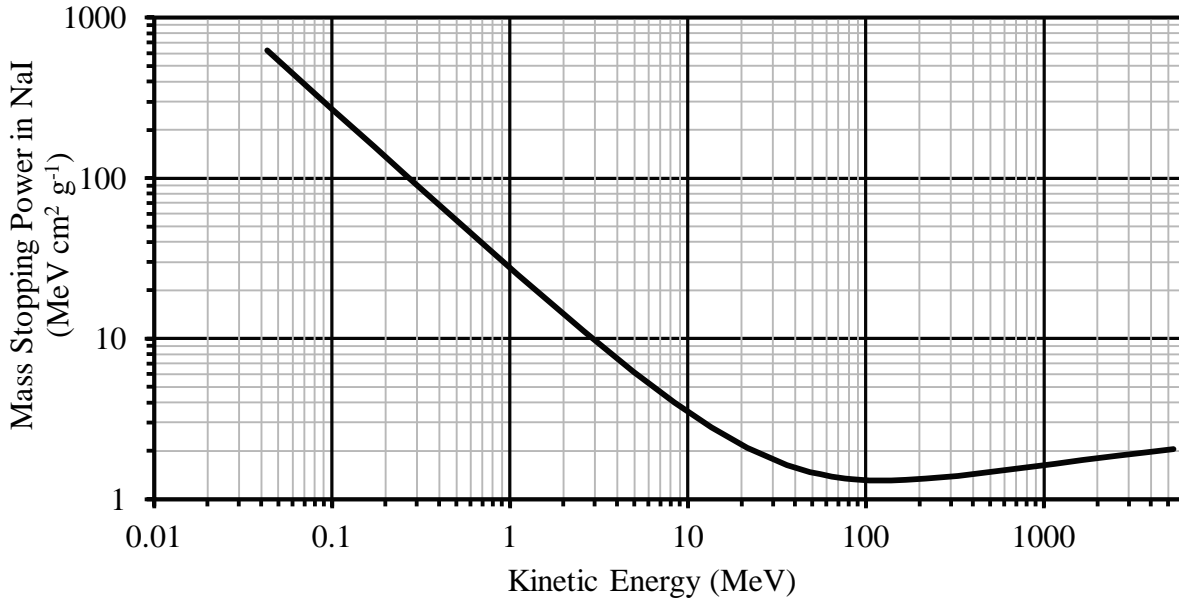


**Figure 4.** Mass stopping power for muons in NaI(Tl) from equation 4.7 of Turner (1992)

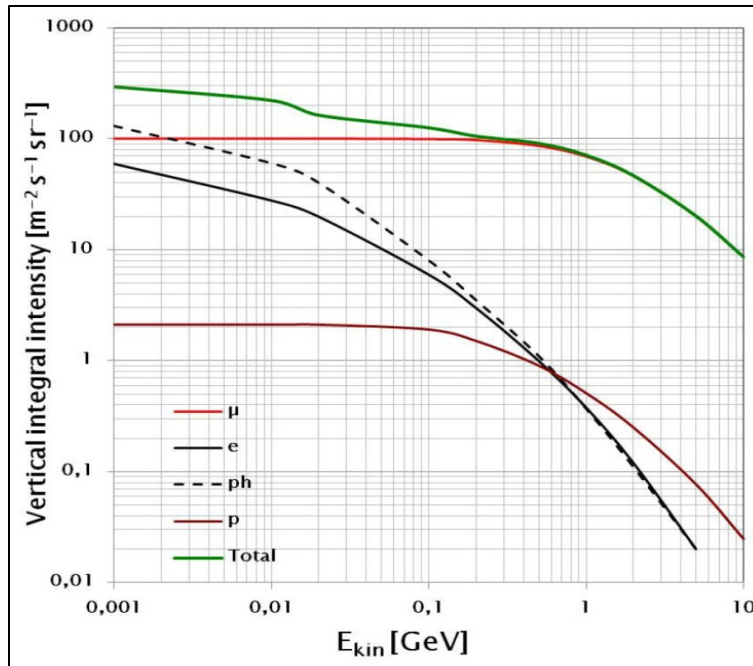


**Figure 5.** Integral fluxes averaged over the 11-year solar cycle for muons ( $\mu$ ), electrons ( $e$ ), protons ( $p$ ), and photons ( $ph$ ) arriving at geomagnetic latitudes  $\sim 40^\circ$  vs. their kinetic energy, Figure 1 from Cecchini and Spuiro (2012).

Cosmic muons have an average energy at sea level of about 4 GeV and a mass stopping power that is a little higher than the minimum at about  $2 \text{ MeV cm}^2 \text{ g}^{-1}$ , as shown in Figure 5. Similarly, while not shown in Figure 5, pions and protons have near minimum mass stopping powers for kinetic energies across a broad range from 0.2–5 GeV. NaI(Tl) has a density of  $3.667 \text{ g cm}^{-3}$  and an estimated minimum mass stopping power of  $1.305 \text{ MeV cm}^2 \text{ g}^{-1}$  for muons, based on the work of Groom et al. (2001). For this combination of mass stopping power and density, the linear energy transfer (LET) is  $4.8 \text{ MeV cm}^{-1}$  and is proportional to the path length of the muon in the detector's active volume. Due to the size and density of the NaI(Tl), energy deposition is assumed to be equal to the energy transferred.

Borak (2012) provided a cumulative probability distribution for random particle traversal path lengths in right circular cylinders of height equal to diameter, as shown in Figure 6. On the plot,  $L$  is particle traversal path length and is related to the diameter of the cylinder,  $D$ , as a ratio:  $L/D$ . This ratio forms the abscissa of the plot, with the ordinate being the probability that  $L/D$  is less than the ratio. This plot is based on a right circular cylinder of height equal to the diameter, where the maximum  $L$  is  $D \times \sqrt{2}$ , and the maximum ratio on the abscissa is  $\sqrt{2}$ , or 1.414.

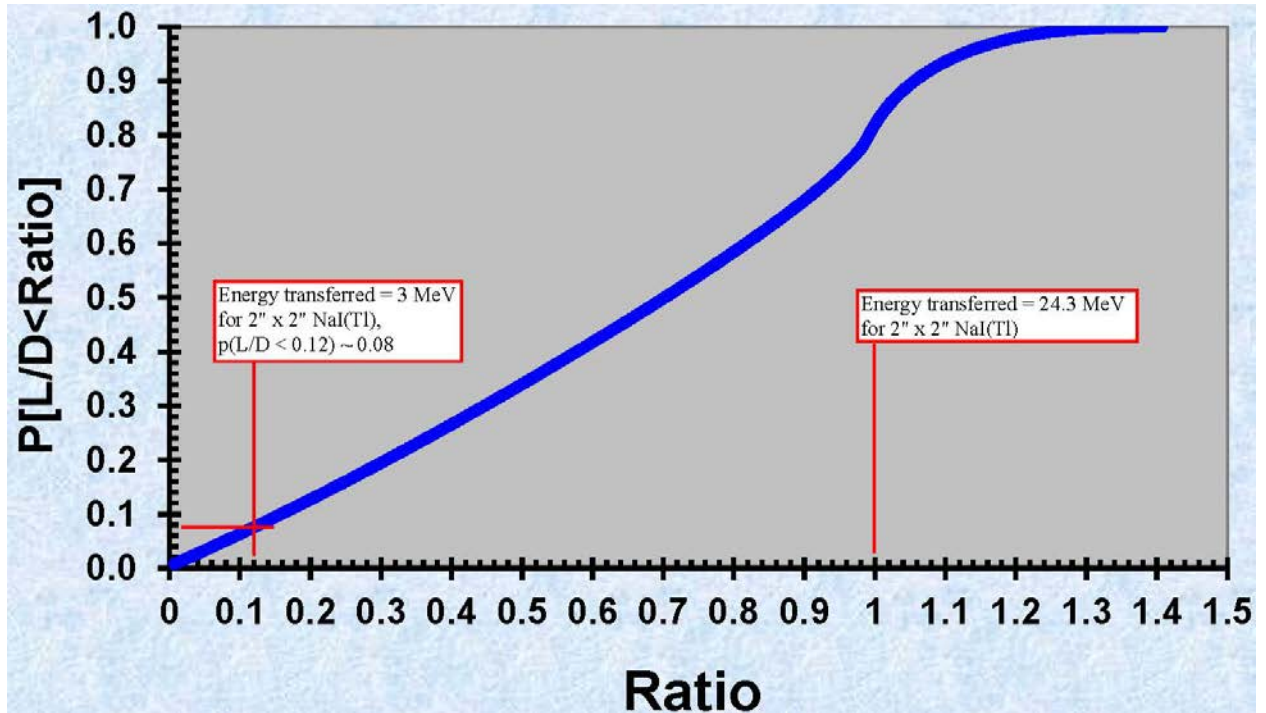


**Figure 6. Cumulative distribution function (CDF) for random particle transversals through a right circular cylinder of height and diameter = 5.08 cm, and ratio of path length,  $L$ , to diameter,  $D$**

[CDF courtesy of Borak (2012) based on the method described in Borak (1994).]

For an industry-common 2 inch by 2 inch NaI(Tl) detector, using the minimum mass stopping power of a muon traversing the cylinder parallel to its axis, i.e.,  $L = D = 2 \text{ inch}$  (5.08 cm), the energy transfer would be  $(4.8 \text{ MeV cm}^{-1} \times 5.08 \text{ cm}) = 24.3 \text{ MeV}$ . Figure 7 illustrates a particle traversal of this type as event #1. In addition, Figure 7, displays the energy



transferred for this case, ratio = 1. Event #2 in Figure 7 depicts a particle traversal at the longest possible path length through the cylinder, ( $5.08 \text{ cm} \times \sqrt{2}$ ), or 7.18 cm. For a muon of minimum stopping power, the energy transfer would be 34.4 MeV, although for a muon with kinetic energy of 4 GeV, the energy transfer would about 53 MeV. Event #3 depicts a particle traversal that grazes the edge of the cylinder, and has a very short path length compared to the other two, with proportionately lower energy transfer than the other two particle traversals if all three have the same stopping power. Event #4 depicts a photoelectric interaction of an incident photon in the detector volume. In contrast to the charged particle traversals in events 1 to 3, the electron depicted in the event has a short range. This is expected for secondary electrons created by interactions of photons emitted in the radioactive decay of environmental radionuclides. A 3-MeV electron has a maximum range in NaI(Tl) of about 0.55 cm, and a large majority of electrons of this energy created in a 2 inch by 2 inch NaI(Tl) detector would exhibit full transfer of energy to the crystal.

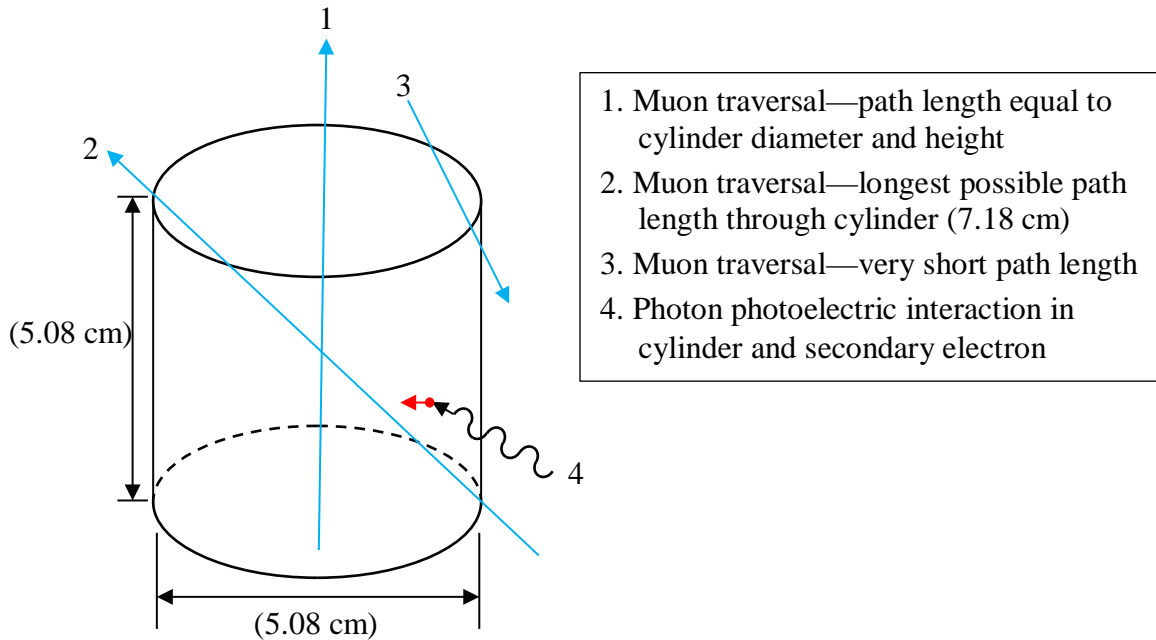


**Figure 7. Example photon interaction and muon traversals through right circular cylinder with diameter and height equal to 5.08 cm, i.e., 2 inch by 2 inch**

Because the range of stopping powers of cosmic muons in NaI(Tl) is small, the greatest source of variability in the energy transferred per traversal in the detector is attributed to the path length. For a 3-MeV maximum energy acceptance, per Figure 6, only eight percent of random, minimally-ionizing, muon particle traversals would transfer energy sufficiently low for acceptance. The average energy transfer of minimally ionizing muons below the 3-MeV threshold is about 1.5 MeV, whereas the average energy transfer for all randomly traversing minimally-ionizing muons in the NaI(Tl) is 16.2 MeV. Subsequently, because only about eight percent of the minimally-ionizing muons traversing the active volume of the detector have energy transfers below 3 MeV, and the average energy transfer of these muon traversals is less than 10% of the average transferred by all muon traversals, less than 1% of the energy

transferred by muons to the detector is quantified. This is visually represented by the area under the CDF in Figure 6—integrated between ratio values of 0 and 0.12. The disparity in quantified interactions versus those truncated is even more pronounced for cosmic muon interactions that have a higher stopping power. A similar argument can be made for cosmic pions and protons as each has a similar, minimally-ionizing stopping power in NaI(Tl), although in terms of flux density, pions and protons are significantly lower in abundance at sea level than muons. With respect to neutrons, ion chambers and NaI(Tl) detectors have an insignificant response. Evaluations of electron and photon interactions are more complex. Due to the generally lower energy of the photon and electron distributions compared to muons, pions, and protons, a much larger fraction of interaction events in NaI(Tl) will have energy transfers below the 3-MeV threshold. Electrons and photons are the only group of cosmic particles that have appreciable quantification in the NaI(Tl) below 3 MeV per energy transfer event. Due to the low contribution to dose compared to other cosmic particles at sea level, a detailed analysis is not provided here.

Table 4 contains the data from Table 1 modified for the anticipated response of an ion chamber and a 2 inch by 2 inch NaI(Tl). Due to the modified response, i.e., the 3-MeV threshold of the NaI(Tl) to muons, pions, and protons, the response of this detector is dominated by its response to photons and electrons. Two simplifying assumptions were made in the calculations.

**Table 4. Data from Table 2 modified with respective detector response characteristics**

Radiation Type	Ion Chamber Reported Output ( $\mu\text{Sv h}^{-1}$ )				NaI(Tl) Detector Reported Output ( $\mu\text{Gy h}^{-1}$ )			
	Sea-Level	2,500 ft	5,000 ft	7,500 ft	Sea-Level	2,500 ft	5,000 ft	7,500 ft
Muons	0.027	0.031	0.036	0.0405	0.00027	0.00031	0.00036	0.000405
Pions	-*	-	0.00066	0.0011	-	-	-	-
Protons	0.0002	0.0006	0.00135	0.0025	-	-	-	-
Photons & Electrons	0.0042	0.0069	0.01	0.013	0.0042	0.0069	0.01	0.013
Neutrons	-	-	-	-	-	-	-	-
Total	0.0314	0.0385	0.0474	0.0560	0.0045	0.0072	0.010	0.013

\* Negligible

Because of the modified detector response to muons, pions, and protons, NaI(Tl) was assumed to quantify only 1% of the energy transferred by these particles, whereas the actual value is lower. As well, no reduction in response to electrons and photons in the NaI(Tl) was assumed, though some energy transfer events would be truncated. The plots in Figure 8 show the relative predicted response of the two detector types to cosmic radiation in the presence of three different levels of terrestrial radiation. The ratios between the responses of an ion chamber and NaI(Tl) are notably dependent on the level of terrestrial radiation. For the lowest level of terrestrial radiation displayed,  $0.02 \mu\text{Gy h}^{-1}$ , the disparity between the responses of the two detector types is greater than two-fold across the range of altitudes evaluated. The Aomori Prefecture MEXT station had an assumed pre-accident dose rate of  $0.02 \mu\text{Gy h}^{-1}$  and is consistent with a dose from only a terrestrial source, as estimated by Minato (2006). Data from this MEXT location was modified by a factor of 5.12 to more closely correspond to DOD/DOE measurements (Cassata et al. 2012). In contrast, the Yamagata MEXT

station (elevation ~ 1,740 ft) had a much higher mean terrestrial dose rate,  $0.0933\mu\text{Gy h}^{-1}$ , and had an adjustment factor of only 1.90 applied to its data (Cassata et al. 2012).

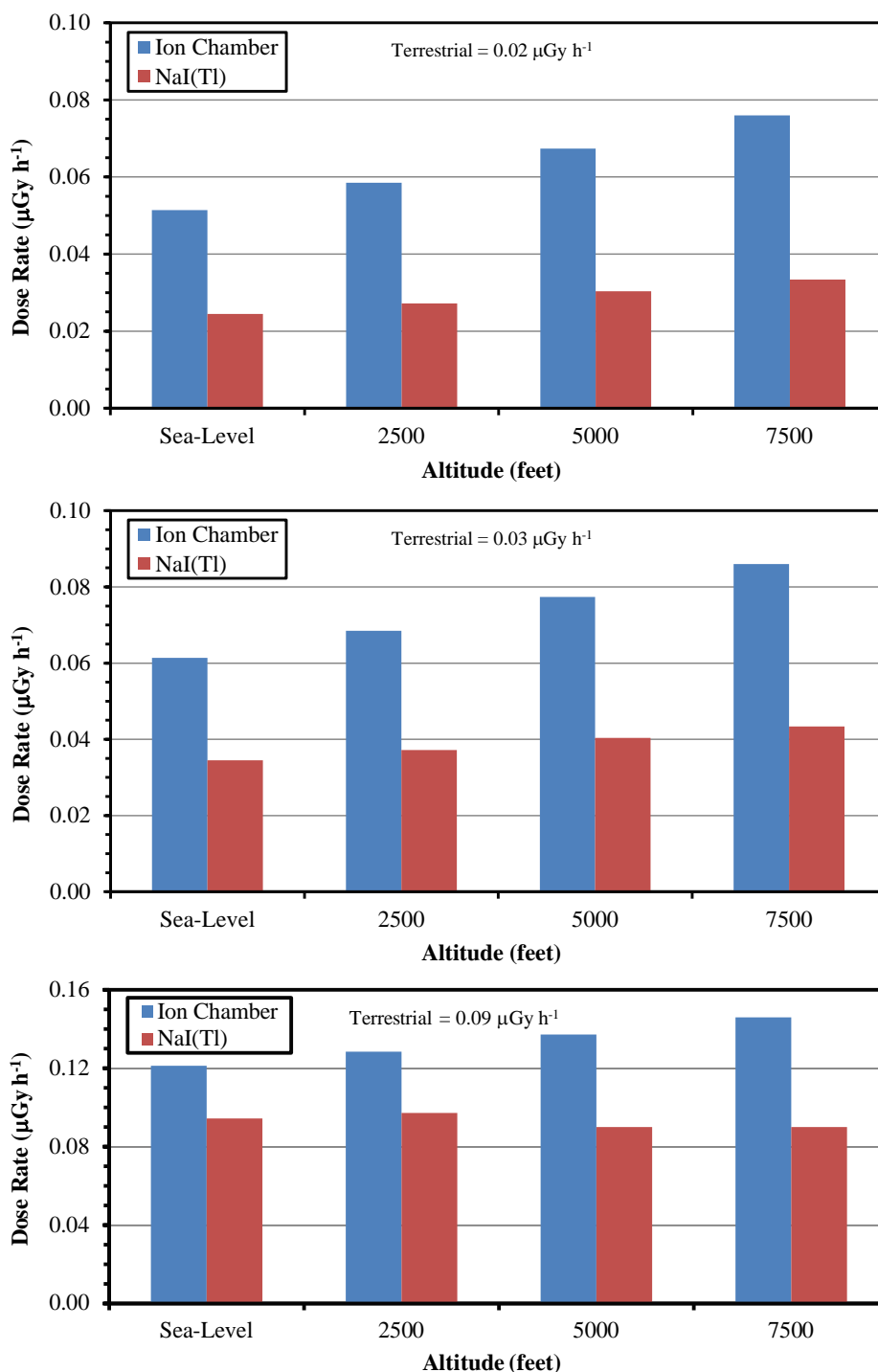


**Figure 8. Estimated differences in external dose rates of an ion chamber and a 2 inch by 2 inch NaI(Tl) for fixed cosmic radiation levels at four altitudes in the presence of three different terrestrial contributions**

In this case, the adjustment for differences in response of DOD/DOE and MEXT detection systems to cosmic radiation was much lower than that for Aomori Prefecture, as depicted in the comparisons made in the third plot of Figure 8. This analysis did not include the contributions of fallout from the FDNPS to the terrestrial radiation component. For some measurement locations that were significantly impacted by fallout, it would be important to include fallout in this analysis. However, for the MEXT data from Aomori and Yamagata Prefectures, impacts of fallout on the terrestrial dose levels were small. For many of the MEXT measurement locations on Honshu Island that were important to DOD use, terrestrial radiation levels were fairly low. As such, the differences in the response of measurements conducted by the DOD/DOE and MEXT were appreciable, especially for locations that did not have significant contributions from ground-deposited fallout. While this difference could have been accounted for if background assessments had been completed before the accident for both instrument types, the DOD and DOE did not collect pre-accident measurements. It is important to note that the DARWG used ratio values to modify MEXT measurement data prior to augmentation with DOD and DOE data in the calculation of estimated doses. While the most appropriate method to correct for the omission of cosmic contributions in MEXT data would have been the addition of an estimated cosmic contribution rather than using a multiplication factor, this was done knowingly and is considered to result in conservative dose estimates.

## **Section 4.**

### **Conclusions**

MEXT and many other Japanese entities use NaI(Tl) scintillator detectors for monitoring of external radiation. Radiation measurements from these instruments, especially those at fixed monitoring locations, were vital to the DOD in assessment of external radiation dose potential to its service men and women, and affiliated civilians and dependents. MEXT data were used to augment DOD measurements, as the DOD did not have external dose measurements at some installations shortly after the accident and the DOD measurements were not conducted continuously as were the measurements at MEXT monitoring stations. However, differences in the measurement techniques and types of instrument used led to differences in the reported dose rates, which were attributed to three sources, namely, the height of detectors above ground, operator interpretation of digital displays, and contributions to dose from the cosmic spectrum, which is addressed herein.

MEXT and many other Japanese entities used NaI(Tl) detectors, but included assessment of only events with energy depositions below 3 MeV, which effectively excluded the majority of dose from directly ionizing cosmic particles and photons. In contrast, the energy-compensated GM's and PICs used by the DOD and DOE included directly ionizing cosmic particles and photons in their dose measurements. As shown in this paper, at measurement locations with terrestrial dose rates equal to  $0.02 \mu\text{Gy h}^{-1}$ , the disparity between the response of the two detectors is over two-fold across the range of altitudes evaluated.

## Section 5.

### References

- Borak, Thomas B., 1994. "A Method of Computing Random Pathlength Distributions in Geometrical Objects," *Radiat Res*, Volume 137, pp. 346–351.
- Borak, Thomas B., 2012. Personal Communication, March 5.
- Cassata, J., Falo, G., Rademacher, S., Alleman, L., Rosser, C., Dunavant, J., Case, D., Blake, P. 2012. *Radiation Dose Assessments for Shore-Based Individuals in Operation Tomodachi, Revision 1*, Report DTRA-TR-12-001 (R1), Defense Threat Reduction Agency, 8725 John J. Kingman Road, Fort Belvoir, VA. December.
- Cecchini, S. and Spurio, M., 2012. "Atmospheric Muons: Experimental Aspects," International Workshop on Muon and Neutrino Radiography 2012, Clermont Ferrand, France, arXiv:1208.1171v1 [astro-ph.EP], April.
- Chikasawa, K., Ishii, T., Sugiyama, H., 2001. "Terrestrial Gamma Radiation in Kochi Prefecture, Japan," *J Health Sci*, Vol. 47, No. 4, pp. 362–372.
- Goldhagen, P., 2000. "Overview of Aircraft Radiation Exposure," *Health Phys*, Vol. 79, No. 5, pp. 526–544. November.
- Groom, D. E., Mikhov, N. V., Stringanov, S. I. 2001. *Muon Stopping Power and Range Tables - 10 MeV - 100 TeV*," Lawrence Berkeley National Laboratory Report 44742, Atomic and Nuclear Data Tables, Vol. 76, No. 2. July.
- Minato, S., 2006. "Distribution of Terrestrial  $\gamma$  Ray Dose Rates in Japan," *J Geogr*, Vol. 115(1), pp. 87–95.
- Nagaoka, K.; Sato, S.; Araki, S.; Ohta, Y.; Ikeuchi, Y.; 2012. "Changes of Radionuclides in the Environment in Chiba, Japan, after the Fukushima Nuclear Power Plant Accident," *Health Phys*, Vol. 102, No. 4, pp. 437–442.
- Nagaoka, K., 2008. "Nationwide Measurements of Cosmic-Ray Dose Rates Throughout Japan," *Radiat Prot Dosim*, Vol. 132, No. 4, pp. 365–374.
- Nagaoka, T., 1987. "Intercomparison between EML Method and JAERI Method for the Measurement of Environmental Gamma Ray Exposure Rates," *Radiat Prot Dosim*, Vol. 18, No. 2, pp. 81–88.
- NCRP (National Council on Radiation Protection and Measurements) 1993. *Report 116—Limitation of Exposure to Ionizing Radiation (Supersedes NCRP Report No. 91)*. NCRP, 7910 Woodmont Avenue, Suite 400, Bethesda, MD.
- Turner, J. E., 1992. *Atoms, Radiation, and Radiation Protection*. McGraw Hill, Inc, New York.